Identification of a Crucial Energetic Footprint on the α1 Helix of Human Histocompatibility Leukocyte Antigen (HLA)-A2 That Provides Functional Interactions for Recognition by Tax Peptide/HLA-A2–specific T Cell Receptors

By Brian M. Baker,* Richard V. Turner,§ Susan J. Gagnon,§ Don C. Wiley,*‡ and William E. Biddison§

*From the *Department of Molecular and Cellular Biology, Harvard University, Cambridge, Massachusetts 02138; the ‡Howard Hughes Medical Institute, Cambridge, Massachusetts 02138; and the §Molecular Immunology Section, Neuroimmunology Branch, National Institute of Neurological Disorders and Stroke, National Institutes of Health, Bethesda, Maryland 20892*

Abstract

Structural studies have shown that class I major histocompatibility complex (MHC)-restricted peptide-specific T cell receptor (TCR)-α/βs make multiple contacts with the α1 and α2 helices of the MHC, but it is unclear which or how many of these interactions contribute to functional binding. We have addressed this question by performing single amino acid mutagenesis of the 15 TCR contact sites on the human histocompatibility leukocyte antigen (HLA)-A2 molecule recognized by the A6 TCR specific for the Tax peptide presented by HLA-A2. The results demonstrate that mutagenesis of only three amino acids (R65, K66, and A69) that are clustered on the α1 helix affected T cell recognition of the Tax/HLA-A2 complex. At least one of these three mutants affected T cell recognition by every member of a large panel of Tax/HLA-A2–specific T cell lines. Biacore measurements showed that these three HLA-A2 mutations also altered A6 TCR binding kinetics, reducing binding affinity. These results show that for Tax/HLA-A2–specific TCRs, there is a location on the central portion of the α1 helix that provides interactions crucial to their function with the MHC molecule.

Key words: T cell receptor • major histocompatibility complex class I–peptide complex • T cell activation • $CD8^+$ T cell • binding kinetics

Introduction

The TCR-α/β determines the specificity of T cell responses. This specificity is for regions of the MHC molecule as well as for the peptide bound in the peptide binding groove of the MHC molecule. Structural studies have shown that the TCR binds to the MHC/peptide complex in a diagonal mode that permits the interaction of CDR loops with both the peptide and the MHC molecule (1–8). For T cells that recognize class I MHC/peptide complexes, amino acids that compose the variable regions of the α and β chains of the TCR make multiple contacts with both the α1 and α2 helices of the MHC (1–7).

The first structure of a human TCR-α/β/peptide/MHC complex to be determined was the A6 TCR specific for the human T lymphotropic virus type I Tax peptide (LLFGYPVYV) presented by HLA-A2 (2). The A6 TCR buries a total of 1,031 $Å^2$ of solvent accessible surface area of the Tax/HLA-A2 complex (2). Of this total buried surface area, 695 $Å^2$ or 67% of that area is HLA-A2 alone. 15 amino acids on HLA-A2 are contacted by the A6 TCR, 6 on the α1, and 9 on the α2 helices. Although the high resolution structure of the A6 TCR/Tax peptide/HLA-A2 complex provides a clear picture of the interface between these proteins, it does not provide direct information about the contributions of the various TCR-peptide/MHC contacts. Conceptually, there are two possibilities: (a) the binding free energy between the two proteins could be generated by only a few strong interactions; or (b) accumulation of many weaker contacts over the entire interface could provide the necessary binding energy. It is currently unknown whether one or both of these possibilities applies.

Address correspondence to W.E. Biddison, National Institutes of Health, Bldg. 10, Rm. 5B-16, Bethesda, MD 20892. Phone: 301-496-9009; Fax: 301-402-0373; E-mail: web@helix.nih.gov

Many studies have examined the effects of MHC mutations on TCR recognition (e.g., 9–11), but none of these MHC mutant studies have had the advantage of being able to precisely target and isolate the TCR contact residues identified by a high resolution structure of the trimolecular complex.

In this study, we have used the knowledge of the TCR contacts between the A6 TCR and HLA-A2 (2) to perform alanine scanning mutagenesis of the HLA-A2 contact residues to determine whether a few key residues provided most of the required interactions, or whether there were many amino acids on both helices provided these interactions. The rationale for performing alanine substitutions is that this protocol deletes all interactions made by atoms beyond the β carbon and provides an estimate of the contribution to binding energy made by the missing portion of the side chain (12). The mutant HLA-A2 molecules with substitutions in each of these 15 TCR contacts were then compared with wild-type HLA-A2 molecules for their capacity to present the Tax peptide to A6 TCR-bearing clones. The affinity of soluble A6 TCR for soluble wild-type and mutant HLA-A2/Tax complexes was measured by Biacore (surface plasmon resonance) to more precisely quantitate the effects of the mutations on TCR binding.

Materials and Methods

Generation and Expression of HLA-A2 Mutant Transfectants. The full-length HLA-A*0201 cDNA construct RSV/HLA-A2 (13) was used as a template for mutagenesis by the method of Ho et al. (14). The full-length template was obtained by PCR using the following primers: 5′-TGGGCTGCAGGTCGACTCTAGAGGAT-3′ and 5′-GCCCGGATCCTCTCAGTCCCTCACAAGGCAGC-3′ obtained from Genset. The PCR product was treated with SalI and BamHI (sites underlined), purified, and ligated into the RSV.5neo mammalian expression plasmid (15). Automated DNA sequencing was performed at this stage to confirm the results of mutagenesis by the National Institute of Neurological Disorders and Stroke DNA Sequencing Facility. HMy2.C1R cells (16) were transfected with full-length RSV/HLA-A2 constructs by Lipofectin (Life Technologies). Clones were assayed for surface expression using the anti–HLA-A2 antibodies BB7.2 and MA2.1 (17–20) with a FACSCalibur™ (Becton Dickinson).

Production and Isolation of Soluble Mutant HLA-A2 Heavy Chains. A soluble form of the HLA-A2 heavy chain was produced by the pHN1$^+$/HLA-A201 cDNA construct that encodes amino acids 1–275 of the heavy chain (21). Mutagenesis was performed as described above for the full-length constructs, and the PCR product was generated using the following primers: 5′-ACACAGGAAACAGAATTCAGGAGGAAT-3′ and 5′-GCCAAAACAGAAGCTTTCACTCCCATCT-3′. The PCR product was treated with EcoRI and HindIII (sites underlined), purified, and ligated into the pHN1$^+$ bacterial expression plasmid (22). XL-1 Blue competent bacteria (Stratagene) were transformed with HLA-A2/pHN1$^+$ constructs, and colonies were selected and DNA isolated; the presence of constructs was confirmed by restriction enzyme analysis, and DNA sequencing performed as described above. Positive clones were grown in 6 liter volumes and inclusion bodies containing the soluble HLA heavy chains were isolated (23). The presence of HLA heavy chains was confirmed by SDS/PAGE.

Generation of Soluble HLA-A2/β2m/Tax Peptide and A6 TCR-α/β Complexes. Soluble forms of the HLA-A2/Tax peptide complexes and the A6 TCR-α/β were refolded from purified inclusion bodies as described (21, 23). In brief, for HLA-A2/Tax, HLA-A2 heavy chain and β2m inclusion bodies were rapidly diluted into a refolding solution (final concentrations 1 μM heavy chain and 2 μM β2m) containing an excess (30 μM) Tax peptide. For the A6 TCR, α and β chain inclusion bodies were rapidly diluted into refolding buffer (final concentrations of 2 μM). After incubation at 4°C for ~24 h, refolded protein was concentrated and purified via size-exclusion chromatography. The A6 TCR construct used contains the α and β chains up to, and including, the cysteines encoding the interchain disulfide bond, followed by a heterodimeric coiled-coil (24) to stabilize the αβ dimer during refolding and analysis. A single free cysteine was added to the COOH terminus of the β chain construct for coupling to a Biacore chip (5).

Biacore Measurements. Biacore measurements were performed on Biacore 1000 and 2000 instruments (Biacore, Inc.) as described previously (5). In brief, the TCR was attached to a CM5 sensor chip using the free cysteine engineered at the COOH terminus of the β chain using thiol coupling. Steady-state equilibrium experiments were performed by injecting 70 μl of HLA-A2/Tax at a flow rate of 10 μl/min. The response was determined by averaging the signal over the final 15 s of the injection and subtracting the response from an identical injection over a mock cysteine-coupled flowcell. Equilibrium response versus injected concentration data were fit to a 1:1 binding model. For kinetic experiments, 60 μl of MHC/peptide was injected at a flow rate of 100 μl/min. Identical injections over the mock flowcell were subtracted from the data. The entire association and dissociation phases were fit to a 1:1 binding model excluding ~2 s at the beginning of each phase. As with our previous studies, we included a term for a small baseline drift during fitting (5). Inclusion of this term, which typically amounted to 1–3% of the total binding response, improved the pattern of the residuals, but had only a minor effect on the fitted parameters. Solution conditions for all experiments were 10 mM Hepes, 150 mM NaCl, 3 mM EDTA, 0.005% polysorbate-20, pH 7.4, 25°C. All injections were repeated twice. Analysis was performed using Biavaluation 3.0 (Biacore, Inc.). For the equilibrium experiments, errors in Table II are the standard fitting error. Errors in kinetic constants are standard deviations from multiple determinations. Errors in k_{off}/k_{on} and $t_{1/2}$ values are derived from the errors in k_{on} and k_{off} using statistical error propagation. HLA-A2/Tax concentrations were determined using an extinction coefficient of 95,839 $M^{-1}cm^{-1}$ (5); this coefficient was reduced by 5,500 for the mutant W167A (25). Concentrations used were the average of three independent dilutions.

T Cell Assays. A6-TCR CD8$^+$ T cell clones 2G4 and RS56 (26) and the B7-TCR T cell clone 10B7 (4) are specific for HTLV-I Tax 11-19 (LLFGYPVYV) presented by HLA-A2. Additional Tax-specific CTL lines were generated from the CD8$^+$ PBL of five additional HLA-A2$^+$ HAM/TSP patients as described previously (26). T cell lines specific for influenza virus matrix peptide M1 58–66 (GILGFVFTL) presented by HLA-A2 (27) were generated from CD8$^+$ PBLs of normal HLA-A2$^+$ donors as described (28). HLA-A2 allospecific CD8$^+$ CTL lines were selected by limiting dilution from a mixed lymphocyte culture of responder PBLs (HLA-A1, HLA-A3, HLA-B14, and HLA-B44) and irradiated stimulator PBLs (HLA-A1, HLA-A201, HLA-B44, and HLA-B55) as described previously (29). Cytotoxicity assays and quantitation of secretion of IFN-γ and

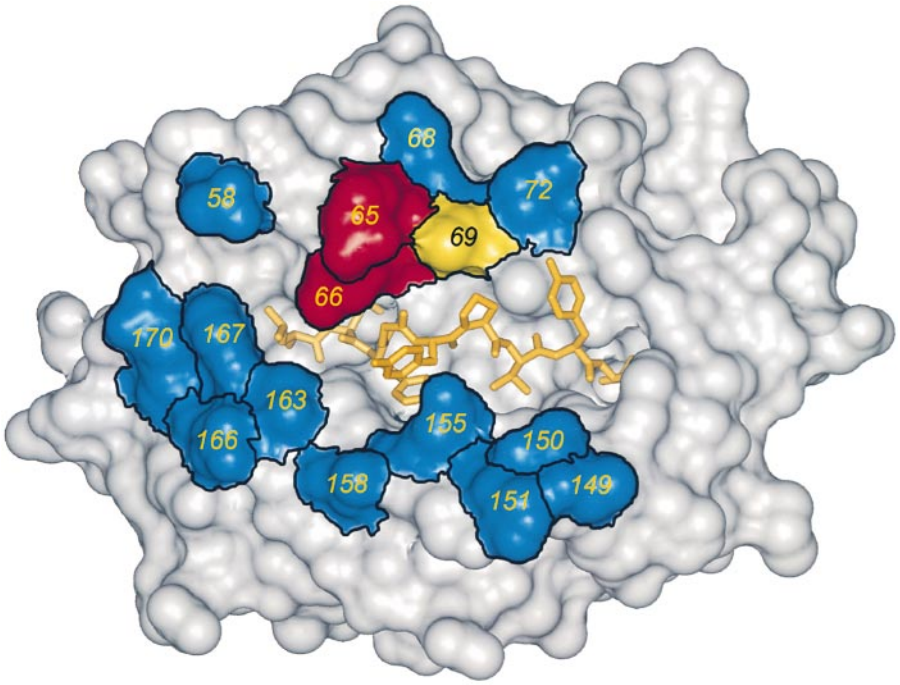

Figure 1. Mutated HLA-A2 amino acids mapped on the surface of the molecule. Coloring indicates the effects of each mutation upon function. Blue, no effect; red, strong effect; yellow, intermediate effect. See Table I for details. Image generated with InsightII (MSI Inc.).

macrophage inflammatory protein (MIP)[1]-1β were performed as described (4). Antigen-presenting cells were HLA-A2 or HLA-A3 transfected Hmy2.C1R cells (16). Tyrosine phosphorylation of TCR-associated ζ-chains and ZAP-70 was quantitated by immunoprecipitation with a polyclonal rabbit anti–ZAP-70 (supplied by Dr. L. Samelson, National Institutes of Health, Bethesda, MD) and immunoblotting with the antiphosphotyrosine antibody 4G10 (Upstate Biotechnology), as described previously (4).

Circular Dichroism Temperature Melts. The thermal stability of peptide/MHC complexes was monitored by circular dichroism (CD) spectroscopy (30, 31) using a Jasco J-710 instrument equipped with a Peltier temperature regulator. Solution conditions were 10 mM sodium phosphate, 10 mM NaCl, pH 7.4. Protein concentrations were ~0.15 mg/ml. Denaturation was monitored at the minimum of 218 nm between 25 and 90°C using a gradient of 1°C/min. Rather than constraining the data to a two-state unfolding model, the data in the transition region were fit to a 9-order polynomial equation and the apparent melting temperature (T_m) determined from the maximum of the first derivative of the fitted curve. The reported T_m values and associated error are averages and standard deviations from three repeated measurements with fresh samples.

Results

Mutation of A6 TCR Contacts with HLA-A2. The crystallographic structure of the trimolecular complex of the A6 TCR-α/β bound to HTLV-I Tax 11–19 peptide/HLA-A2 revealed that this TCR contacted 15 amino acids on the HLA-A2 molecule (reference 2; Fig. 1, and Table I; contacts tabulated with a 4Å distance cutoff). Six of these amino acids were on the α1 helix of HLA-A2 (E58, R65, K66, K68, A69, and Q72), and the remaining nine were on the α2 helix (Table I). Nine of the HLA-A2 amino acids contacted by the A6 TCR were conserved among HLA class I alleles, and six were variable (32; Table I). To examine the functional contributions of these amino acids, and to

Table I. *Summary of A6 TCR Interactions with HLA-A2*

HLA-A2 residue (conserved vs. variable)	HLA-A2 residue contacted by A6 TCR	Mutant HLA-A2 produced	Negative effect on Tax presentation*
Conserved	E58	E58A	−
Variable	R65	R65A	++
Variable	K66	K66A	++
Conserved	K68	K68A	−
Variable	A69	A69G	+
Conserved	Q72	Q72A	−
Conserved	A149	A149G	−
Conserved	A150	A150G	−
Variable	H151	H151A	−
Conserved	Q155	Q155A	−
Conserved	A158	A158G	−
Variable	T163	T163A	−
Conserved	E166	E166A	−
Variable	W167	W167A	−
Conserved	R170	R170A	−

*Negative effects of mutant HLA-A2 molecules are scored as "−" if they produced a <10-fold reduction in the amount of Tax peptide required to produce 50% of maximum lysis, IFN-γ, and MIP-1β secretion relative to wild-type HLA-A2, "+" if they produced a 10–100-fold reduction in activity, and "++" if they produced a >100-fold reduction in activity.

[1]*Abbreviations used in this paper:* CD, circular dichroism; MIP, macrophage inflammatory protein.

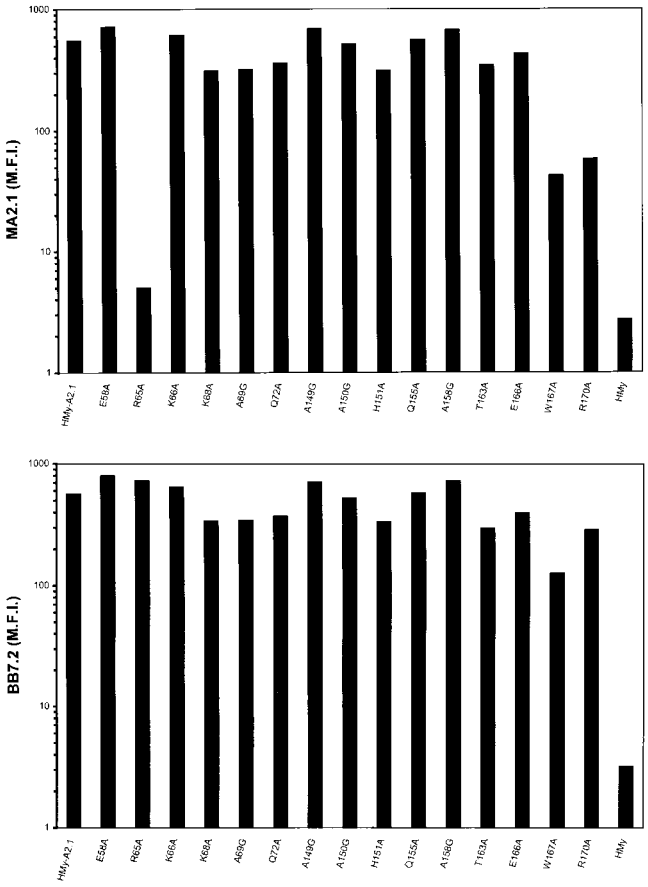

Figure 2. Levels of cell surface expression of wild-type and mutant HLA-A2 molecules. Hmy2.C1R cells were transfected with the indicated mutant HLA-A2 constructs and levels of cell surface expression measured by cytofluorometry using two different anti-A2 antibodies MA2.1 (top) and BB7.2 (bottom). Untransfected cells served as a negative control (Hmy). Y-axes are mean fluorescence intensity (M.F.I.).

determine if one particular area was critical for recognition of the A6 TCR, site-directed mutagenesis was performed on the HLA-A2 cDNA that substituted alanine for each of these amino acid contacts (for cases in which alanine was the contact residue, glycine was substituted for alanine).

Substitution by alanine (or glycine) deletes interactions made by atoms beyond the β carbon and provides an estimate of the contribution to binding energy made by the original side chain (12). Wild-type and mutant HLA-A2 cDNAs were generated that encoded the full-length molecule for transfection into Hmy2.C1R cells (16) and a truncated soluble form for utilization in TCR binding assays (21). Cell surface expression of the mutant HLA-A2 molecules was quantitated by cytofluorometry using two different HLA-A2 monoclonal antibodies that are known to react against different HLA-A2 epitopes (BB7.2 and MA2.1; references 17–20; Fig. 2). Only one of the HLA-A2 mutant transfectants had less than a twofold level of expression relative to wild-type with both of these antibodies (W167A; Fig. 2). Two of the mutants showed decreased reactivity with MA2.1 but not BB7.2 (R65A and R170A; Fig. 2). These results were consistent with previously published findings on the specificity of MA2.1 (17, 19, 20).

A6 TCR-bearing Clonal T Cell Activation by HLA-A2 Contact Mutants. The effects of the HLA-A2 amino acid substitutions on T cell activation were assessed by the capacity of the mutants to present the Tax peptide to the A6 TCR-bearing clones 2G4 and RS56. Activation was measured by a series of T cell effector assays: (a) cytotoxicity of peptide-pulsed target cells; (b) induction of MIP-1β and IFN-γ secretion; and (c) phosphorylation of the TCR-associated ζ-chains and ZAP-70. Representative results are presented in Fig. 3. The only dramatic negative effects produced were the alanine substitutions of R65 and K66, which produced a >1,000-fold reduction in all three T cell effector assays (Fig. 3, A–C), whereas the substitution of A69 with glycine produced a 10–100-fold decrease in the re-

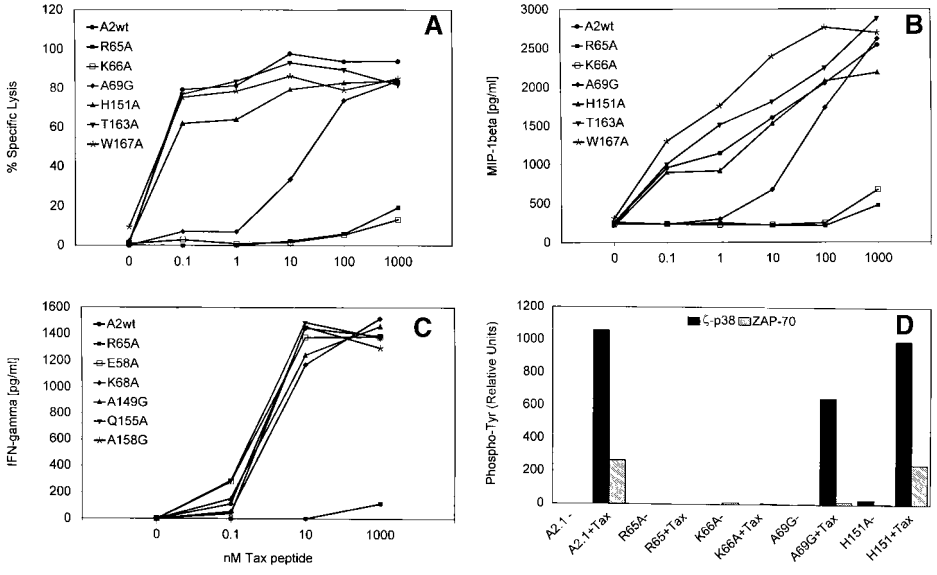

Figure 3. Presentation of the Tax peptide by wild-type and mutant HLA-A2–transfected cells to A6 TCR-bearing clones. Clone 2G4 was assayed for the capacity to recognize Tax peptide-pulsed antigen-presenting cells by (A) direct lysis (E/T ± 2.5:1), (B) MIP-1β secretion, and (C) IFN-γ secretion. (D) A6 TCR-mediated signal transduction was quantitated by phosphorylation of the p38 form of phospho-ζ-chains and phosphorylation of ZAP-70 from clone RS56 stimulated with the indicated unpulsed (−) or Tax peptide-pulsed antigen-presenting cells. In A, additional titrations of 0.01 and 0.001 mM peptide for Tax, H151A, and T163A were indistinguishable, but were not shown because of x-axis compression.

sponses to the Tax peptide (Fig. 3, A and B). All of the other mutants produced less than a 10-fold reduction in the reactivity to the Tax peptide for each of these three assays of T cell activation (Fig. 3, summarized in Table I).

If the negative effects on T cell effector functions produced by the R65A, K66A, and A69G mutations were due to direct effects on TCR binding and signaling, then they should produce changes in the most membrane proximal TCR signaling events of phosphorylation of the TCR-associated ζ-chains and ZAP-70 (33, 34). A6 TCR engagement by wild-type HLA-A2 presentation of the Tax peptide induces the characteristic agonist pattern of p38-ζ and ZAP-70 phosphorylation (Fig. 3 D). Activation by R65A and K66A presentation of the Tax peptide showed no detectable phosphorylation of p38-ζ or ZAP-70 (Fig. 3 D). The A69G mutant that had less of a negative effect on T cell effector function showed a different partial agonist pattern of phosphorylation, with some detectable p38-ζ phosphorylation, but no detectable ZAP-70 phosphorylation (Fig. 3 D). A representative mutant that showed no negative effect on T cell effector functions (H151A) showed a phosphorylation pattern indistinguishable from wild-type HLA-A2 (Fig. 3 D). These results demonstrate that the R65A, K66A, and A69G mutations selectively interfere with A6 TCR recognition and signal transduction induced by Tax/HLA-A2.

Effects of HLA-A2 Mutations on A6 TCR Binding of Soluble Tax/HLA-A2 Complexes. The effects of several of the amino acid substitutions on the kinetics and thermodynamics of the A6 TCR to binding Tax/HLA-A2 complexes were measured using Biacore. The three mutants that demonstrated negative effects on TCR signaling (R65A, K66A, and A69G) were examined, as were three that showed no significant functional effects (T163A, E166A, and W167A). Experiments were performed with the TCR covalently coupled to the sensor chip through an engineered cysteine at the COOH terminus of the β-chain. Both steady-state equilibrium and kinetic Biacore experiments were performed; in each, affinities resulting from the two measurements were similar.

Representative Biacore data are shown in Fig. 4 A; all binding data are summarized in Table II. With one exception, the substitutions resulted in moderate effects on K_D, values ranged from 12.4 μM (A69G) to 2.8 μM (T163A; wild-type HLA-A2/Tax binds the A6 TCR with a K_D of 0.82 μM; reference 5). The single mutation that had a large effect on the K_D was R65A, with a value of 96 μM, ~120-fold weaker than the wild-type.

The mutations resulted in large effects on binding kinetics, with $t_{1/2}$ ranging from 1.0 (A69G) to 13.9 s (K66A; $t_{1/2}$ for the wild-type interaction is 7.5 s; reference 5). The slow dissociation rates for the K66A and R65A mutants are qualitatively apparent in Fig. 4 B. Each substitution also resulted in an apparent decrease in association rate (k_{on}) relative to the wild-type interaction (k_{on} with wild-type HLA-A2 is 1.1×10^5 $M^{-1}s^{-1}$; reference 5). The reductions in k_{on} for the R65A and K66A substitutions are substantial, the respective values of 829 $M^{-1}s^{-1}$ and 3.2×10^3 $M^{-1}s^{-1}$ represent ~133- and ~34-fold decreases relative to wild-type.

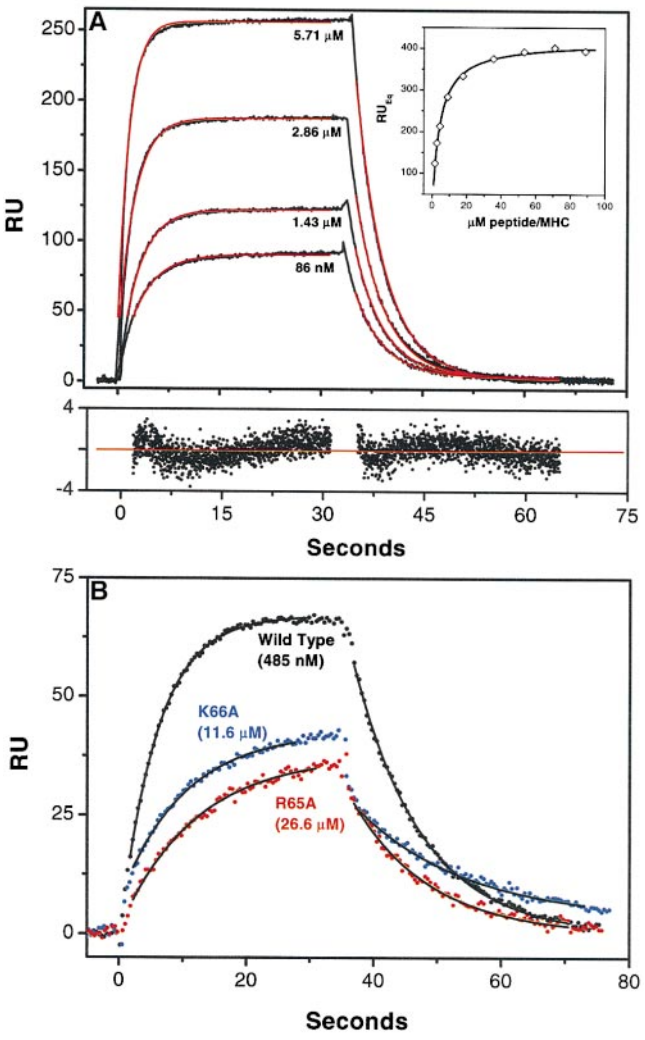

Figure 4. Representative Biacore binding data. (A) Full kinetic dataset for the Tax/HLA-A2 E166A mutant binding immobilized A6 TCR. Red lines represent fits to a 1:1 binding model; injected concentrations are indicated. Residuals are indicated below the data. Inset: separate equilibrium binding experiment for E166A. (B) Representative kinetic traces for wild-type Tax/HLA-A2, the K66A mutant, and the R65A mutant binding to the A6 TCR. The slow dissociation rates for K66A and R65A are apparent. Data are plotted as every fourth data point along with fits to 1:1 binding models. Plots represent one trace from full datasets as in A. Injected TCR concentrations are indicated. RU, reasonable units.

Effects of R65A, K66A, and A69G Mutations on Other Tax/HLA-A2–specific T Cells. To determine if the negative effects of the R65A, K66A, and A69G mutations on recognition of the Tax/HLA-A2 complex by the A6 TCR are generalizable to other Tax/HLA-A2–specific T cells, we assessed the reactivity of the B7 TCR, a second Tax/HLA-A2–specific TCR-α/β, with each of the three mutants. In the crystallographic structure of the B7 TCR complexed with Tax/HLA-A2, Arg65, Lys66, and Ala69 form contacts with this TCR that are very similar to the contacts these amino acids make with the A6 TCR (4).

Table II. *Kinetics and Affinities for HLA-A2/Tax Ligands Binding to A6 TCR at 25°C*

HLA-A2 sequence	k_{on} ($M^{-1}s^{-1}$)	k_{off} (s^{-1})	$t_{1/2}$ (s)*	k_{off}/k_{on} (μM)	$K_{D,eq}$ (μM)	$\triangle G°$ (kcal/mol)‡
Wild-type§	$1.1 \pm 0.1 \times 10^5$	0.093 ± 0.002	7.5 ± 0.2	0.82 ± 0.08	0.91 ± 0.09	8.24
R65A	829 ± 193	0.079 ± 0.002	8.8 ± 0.2	96 ± 22	84 ± 32	5.56
K66A	$3.2 \pm 0.3 \times 10^3$	0.050 ± 0.002	13.9 ± 0.6	15.6 ± 1.2	18.7 ± 7.5	6.45
A69G	$5.5 \pm 0.3 \times 10^4$	0.682 ± 0.026	1.02 ± 0.04	12.4 ± 0.9	9.6 ± 0.4	6.84
T163A	$6.0 \pm 0.2 \times 10^4$	0.168 ± 0.009	4.13 ± 0.22	2.8 ± 0.2	3.1 ± 0.2	7.51
E166A	$4.6 \pm 0.5 \times 10^4$	0.197 ± 0.008	3.51 ± 0.14	4.3 ± 0.2	4.0 ± 0.2	7.36
W167A	$1.2 \pm 0.1 \times 10^5$	0.572 ± 0.023	1.21 ± 0.05	4.8 ± 0.4	6.9 ± 0.4	7.04

*$t_{1/2} = 0.693/k_{off}$.
‡$\triangle G° = -RT\ln K_D$, steady-state equilibrium values.
§From reference 5.

Reactivity of each of the mutants with the B7 TCR was assayed by measuring the ability of the B7 TCR-expressing T cell line 10B7 to lyse peptide-pulsed targets. As shown in Fig. 5, the R65A and K66A mutants had a substantial loss of activity with the B7 TCR that resembles the activity loss with the A6 TCR. In contrast, the A69G mutant did not have a significant effect with the B7 TCR.

To further address the general nature of the negative effects of the R65A, K66A, and A69G mutations on Tax/HLA-A2–specific T cells, we next generated Tax/HLA-A2–specific T cell lines from five additional HLA-$A2^+$ HAM/TSP patients and assayed them for the ability to lyse Tax peptide-pulsed wild-type and mutant HLA-A2 target cells. The results, summarized in Table III, show that of 201 Tax/HLA-A2–specific CTL lines assayed, at least one of these three HLA-A2 mutants produced a negative effect on Tax presentation on all of these CTL lines. Each of the mutants showed no effect on Tax presentation by at least four CTL lines, indicating that none of these three mutants had an intrinsic negative effect on Tax presentation or the ability to bind the Tax peptide. Taken together, these results indicate that the area on the α1 helix of the HLA-A2 molecule encompassing residues R65, K66, and A69 has an important role in recognition of the HLA-A2 molecule by Tax-specific TCRs.

Effects of R65A, K66A, and A69G Mutations on Other, Non-Tax–specific, HLA-A2–restricted/specific T Cells. To determine if all TCRs that recognize HLA-A2 focus on the same α1 helical region (around amino acids R65, K66, and A69), we tested T cell lines specific for influenza virus M1 58–66 presented by HLA-A2 (27) and HLA-A2–specific alloreactive T cell lines derived from a mixed lymphocyte culture reaction (29). 4 of 12 M1 58–66–specific T cell lines and 4 of 11 allospecific T cell lines were not affected by any of the three mutations. Representative results for one line from each group are shown in Fig. 6, A and B. When compared with the results for the Tax/HLA-A2–specific T cell lines (201/201 lines affected by at least one of the three mutations), the results clearly demonstrated that TCRs that are specific for a peptide other than Tax that is presented by HLA-A2 or recognize HLA-A2 as an alloantigen do not focus on the same part of the interface with the HLA-A2 molecule that is the focus of Tax-specific TCRs.

Effects of R65A, K66A, and A69G Mutations on Peptide Binding and Presentation by HLA-A2. Do the R65A, K66A, or A69G mutations affect binding and presentation of the Tax peptide by the HLA-A2 molecule? As demonstrated above, we readily found T cell lines that were unaffected by these mutations, indicating that none of them impair binding or presentation significantly enough to affect T cell activation. Nevertheless, small decreases in peptide affinity not obvious in the cellular assays could influence the Biacore binding measurements by decreasing the concentration of active (i.e., peptide-bound) protein. This question is particularly important for the R65A and K66A mutants which show reduced TCR association rates (Table II).

To assay more directly for effects on peptide binding, we performed circular dichroism temperature melting experiments with the wild-type, R65A, K66A, and A69G Tax/HLA-A2 molecules. Due to linkage between peptide binding and folding of the class I heavy chain, the apparent T_m

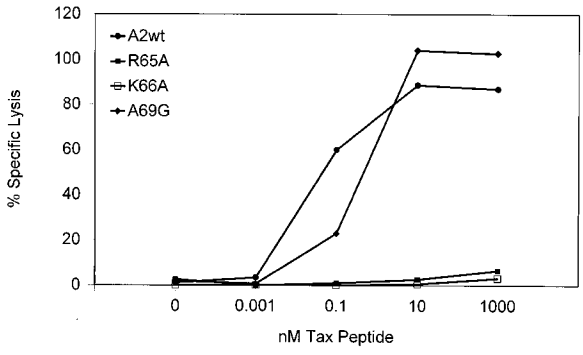

Figure 5. Recognition of Tax/HLA-A2 transfectants by B7-TCR clone 10B7 as measured by cytotoxicity. E/T = 2.5:1.

Table III. *Summary of Anti-Tax CTL Recognition of R65A, K66A, and A69G*

Patient	No. Tax-specific CTL lines	Negatively affected by:* R65A	K66A	A69G
Mu	1	+	+	+
	3	−	+	+
	1	+	+	−
	1	−	+	−
	8	+	+	N.T.
	2	−	+	N.T.
Total	16			
Sa	42	+	+	+
	8	−	+	+
	3	−	+	−
	7	+	+	−
	1	−	−	+
Total	61			
LB	68	N.T.	+	N.T.
JH	3	−	−	+
	1	−	+	+
	2	−	+	−
Total	6			
DL	29	+	+	+
	15	−	+	−
	6	−	+	+
Total	50			
Total	201			

N.T., not tested.
*Negative effects of mutant HLA-A2 molecules are scored as "−" if they produced a <10-fold reduction in the amount of Tax peptide required to produce 50% of maximum lysis relative to wild-type HLA-A2, and "+" if they produced a >10-fold reduction in activity.

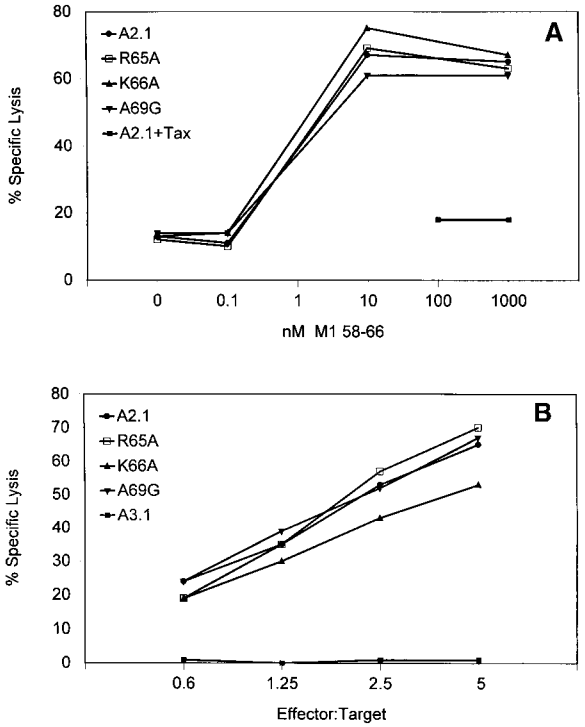

Figure 6. Recognition of HLA-A2 molecules by T cells specific for influenza M1 peptide M1 58–66 and HLA-A2 allospecific T cells. (A) Recognition of M1 peptide-pulsed antigen-presenting cells was assayed by lysis of the M1 peptide-specific CTL line 1E8 at E/T = 5:1. (B) Recognition of unpulsed antigen-presenting cells by the HLA-A2 allospecific T cell line 1C1 at the indicated E/T ratios.

of the peptide/MHC is well correlated with peptide binding affinity (30). The results of these experiments are shown in Fig. 7. As expected, none of the mutations significantly destabilize the molecule. Wild-type Tax/HLA-A2 was found to melt at 65.3 ± 0.3°C, identical to the value previously measured in this laboratory (31). Surprisingly, the R65A mutant had a T_m slightly higher than wild-type (68.3 ± 0.6°C). The K66A mutant was slightly destabilized relative to wild-type (T_m of 63.0 ± 0.3°C), suggesting slightly weaker peptide binding. In other systems, a reduction in T_m of 2.3 degrees is correlated with an ~1 order of magnitude reduction in peptide binding affinity (30). Thus, we cannot rule out the possibility that the slow TCR association rate for K66A is influenced somewhat by weaker peptide binding. The A69G mutant is also slightly destabilized (T_m of 64.1 ± 0.7°C), yet the effects of this mutation on the TCR binding rate are modest (Table II).

Discussion

The Functional and Energetic Footprint of the A6 TCR on Tax/HLA-A2. Wells and colleagues (35–37) have demonstrated by alanine-scanning mutagenesis that dominant contributions to binding energy within protein–protein interfaces tend to cluster in localized regions providing an energetic footprint that is much smaller than the physical footprint of an interaction. In this study, we have performed a similar analysis within the interface between the human class I MHC molecule HLA-A2 complexed with the Tax peptide from the virus HTLV-1 and the human TCR-α/β A6. Initially we examined the functional contributions of the HLA-A2 amino acids contacted by the A6 TCR to T cell receptor signaling. For 12 out of 15 contact residues, substitution with alanine (or glycine) had no significant effect on TCR activity. The only substitutions that did have an effect were R65A, K66A, and, to a lesser ex-

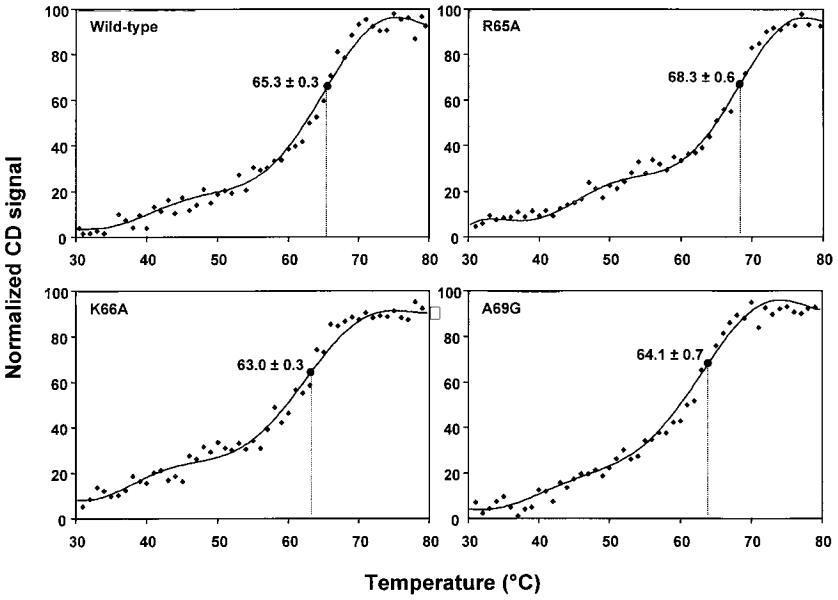

Figure 7. Temperature stability of the wild-type, R65A, K66A, and A69G HLA-A2 molecules with the Tax peptide as measured by CD spectroscopy at 218 nm. The apparent T_m, measured by the inflection point of the fitted curve, is indicated on each plot. Values on the y-axis indicate normalized CD signal.

tent, A69G. These three amino acids lie on the central portion of the α1 helix and form contacts mainly with the CDR3α loop of the A6 TCR (2). Thus, of the HLA-A2 amino acid side chains contacted by the TCR, this region appears to represent an important "footprint" for A6 TCR activity. The contributions from contacts to seven HLA-A2 main chain atoms (involving positions 68, 69, 149, and 150, including hydrogen bonds made with the carbonyl oxygen atoms of A149 and A150) could not be assayed.

Solution binding measurements showed that the three HLA-A2 mutations affecting activity (R65A, K66A, and A69G) also reduce A6 TCR binding affinity. In contrast, measurements for three representative mutations that showed no functional effect (T163A, E166A, and W167A) demonstrated relatively minor effects on TCR binding affinity. These results were not unexpected, as previous studies have shown that reductions in TCR binding affinity resulting from peptide alterations are often associated with losses or decreases in TCR activity (for example, references 5, 38, and 39). The loss in affinity for A69G, which results in weak TCR signaling, is intermediate between the affinity loss for the two mutations which virtually abolish signaling altogether (R65A and K66A) and those that show no functional effect.

Each of the six HLA-A2 mutations assayed in the binding experiments resulted in weaker binding affinity (Table II). Thus, binding energy appears to be distributed somewhat throughout the interface. Yet only the substitutions at positions 65, 66, and 69 reduced affinity (or altered binding kinetics) beyond a "threshold" required for full activity. The $\Delta\Delta G^\circ$ between the weak agonist A69G and full agonist W167A mutants is <1 kcal/mol, and the difference in the half-lives is <1 s (Table II). This illustrates the narrow "window" of physical parameters (measured with soluble molecules at 25°C) that are generally correlated with T cell function (for example, reference 40).

Of the MHC residues contacted by the TCR, Arg65 is one of the few whose side chain is extended fully towards the TCR. The guanidinium group of Arg65 forms a hydrogen bond with the hydroxyl group of Thr98 of the A6 TCR α-chain as well as a salt bridge with the carboxylate of Asp99 (2). Complementary electrostatic interactions across protein interfaces can increase association rates through acceleration of diffusion and electrostatic orientation (41). The interactions with the A6 TCR made by Arg65 may serve such a role, as substitution of Arg65 with alanine reduces the apparent A6 TCR binding rate. However, the ~133-fold reduction is substantial, larger than what is typically observed with electrostatic rate enhancements (for example, reference 42) and there may be other factors contributing to the decrease (see below). Weaker peptide binding is not likely to contribute to this slow rate, as in addition to finding T cell lines unaffected by this mutation (Table III), the R65A molecule has an apparent T_m higher than that of wild-type (Fig. 7).

The dissociation rates (and thus half-lives) for wild-type Tax/HLA-A2 and the R65A mutant are very similar (0.079 s^{-1} for wild-type Tax/HLA-A2 and 0.093 s^{-1} for R65A). The A6 TCR/Tax/HLA-A2 structure does not provide an indication why these values are so similar. Although it is conceptually useful to cast the decrease in association rate as an increase in the height of the transition state barrier to binding (43) this does not provide insight into why the dissociation rates are so similar. Apparently, once the complex has formed, the strength of the intermolecular interactions made with the A6 TCR by wild-type HLA-A2 and the R65A mutant are similar. Structural reorganizations occurring within the interface may result in new interactions that make up for those lost by the R65A mutation. Such reorganizations, if occurring, could also contribute to the slower binding rate, as could any increase in flexibility resulting from the mutation. Modeling or a crystallographic

structure of the complex with the R65A mutant could provide insight into the molecular details underlying the reductions in both association and dissociation rates.

In the TCR/peptide/MHC structure with the Tax/HLA-A2–specific TCR-α/β B7, Arg65 also forms a hydrogen bond and a salt bridge with the B7 TCR α-chain (4). As with the A6 TCR, the R65A substitution significantly reduces cytotoxic activity with B7 TCR-bearing T cells. This finding suggests that Arg65 acts in a similar role for both the A6 and B7 TCRs. However, the contribution of Arg65 cannot be as significant with other Tax/HLA-A2–specific TCRs, as out of an additional 133 T cell lines examined for negative effects with R65A, 45 were not adversely affected. These other TCRs may not have complementary amino acids capable of forming hydrogen bonds or salt bridges with Arg65 in the CDR3α loop and may compensate for the loss of this interaction through other contacts elsewhere in the interface.

The β-carbon of Ala69 forms a single hydrophobic contact with the side chain of Trp101 of the A6 TCR α-chain. Replacement of Ala69 with glycine significantly increases the TCR dissociation rate, resulting in a TCR/peptide/MHC half-life of 1.0 s (Table II; wild-type value is 7.5 s). The increase in k_{off} contributes to a weakening of the TCR binding affinity by approximately one order of magnitude. Although removal of the single hydrophobic contact made by Ala69 likely contributes to the affinity loss, the effect of replacing an alanine with the conformationally less restricted glycine on the local structure of the MHC α1 helix may also have an effect. However, the A69G substitution did not have an adverse effect on activity with the B7 TCR, with which it makes a similar hydrophobic contact, nor did it have an effect on 29 out of 123 additional T cell lines screened.

As opposed to Arg65 and Ala69, the side chain of Lys66 does not protrude from the MHC; rather it lies parallel to the peptide binding groove and helps bury the peptide anchor residue Leu2 (the γ-carbon of the Lys66 side chain also forms hydrophobic contacts with the β- and γ-carbons of Asp99 of the A6 TCR α-chain). As such, Lys66 does not form any direct electrostatic interactions with the A6 TCR. Nevertheless, it still adds to the net charge of the HLA-A2 TCR binding site and may contribute to electrostatic acceleration of the binding rate. Consistent with this hypothesis, the K66A substitution reduces the apparent A6 TCR association rate by 34-fold. Again though, the reduction is large and there may be other factors contributing to the rate decrease (see above). Circular dichroism melting experiments indicate that the K66A mutant melts at a slightly diminished T_m compared with wild-type (Fig. 7), consistent with a reduction in peptide binding affinity. This may contribute somewhat to the apparent decrease in TCR association rate, yet the fact that we were able to find T cell lines unaffected by the K66A mutation (Table III) as well as purify normal quantities of the molecule indicates that the effect on peptide binding is not substantial.

The TCR binding kinetics for K66A indicates that the half-life of the TCR/peptide/MHC complex with the K66A mutant is ~14 s, or almost twice as long as wild-type. As with the R65A mutant, the structure with wild-type HLA-A2 does not provide insight into the reason for this long half-life. In this case, once the complex is formed the intermolecular interactions are stronger than in the wild-type complex. Again, modeling or crystallographic studies of the mutant complex would be insightful.

A Poor Correlation of Activity with TCR/Peptide/MHC Half-Life. In many studies, the half-life of the TCR/peptide/MHC complex is well correlated with activity (39). Nevertheless, despite its long half-life (~14 s), the K66A mutant is almost completely inactive. Likewise, the R65A mutant, which has a TCR/peptide/MHC half-life similar to wild-type (8.8 vs. 7.5 s; Table II), is inactive. As discussed, both mutants bind the A6 TCR slower than wild-type HLA-A2. It is possible that the loss of function observed with these two mutants is due to slow binding rates. If more than one TCR must be engaged within a given time interval for T cell activation to proceed, then the rates at which TCR/peptide/MHC complexes form could influence in the quality or quantity of TCR signaling. A direct correlation with affinity is ruled out, as the K66A mutant binds with an affinity only ~15–20-fold weaker than wild-type, close to the value of A69G (partially active) and in the range of peptide substitutions which are still partial agonists. These two mutants add to a growing list of ligands whose TCR dissociation rates do not correlate with activity (for example, references 38 and 44). Apparently, there are factors other than the half-life of the TCR/peptide/MHC complex that can affect T cell function.

Generality of the Footprint and the Role of the Peptide in Directing TCR Focus. The 65/66/69 region is important for recognition of Tax/HLA-A2 in general, as 201/201 Tax/HLA-A2–specific cell lines were affected by at least one of these substitutions (Table III). However, the fact that not every cell line was equally affected by all three mutations as well as the different response of the A6 and B7 TCRs towards the A69G mutation indicates some Tax/HLA-A2–specific TCRs can better accommodate substitutions in this region. Similar patterns have been observed before: in their mutational analysis, Ono et al. found that different TCRs specific for VSV-based peptides presented by the mouse class I MHC H-2K^b had slightly altered patterns of reactivity towards a panel of MHC mutations, although, as we have observed, certain clusters tended to dominate (45).

In studying the effects of substitutions in the Tax peptide upon recognition by the A6 TCR, Hausmann et al. observed that substitution by alanine for three out of seven nonanchor residues abolished cytotoxic activity (46). Furthermore, alanine substitutions in other positions resulted in an intermediate loss of activity similar to what we have observed here with the A69G mutation. When compared with our observation that alanine substitutions for only 2 out of 15 HLA-A2 residues contacted by the A6 TCR abolish activity as well as the apparent generality of this footprint, this implies that the Tax peptide plays a significant role in influencing the TCR "focus". Finding similar results in a mouse class II MHC system, Ehrich et al. (47)

concluded that the TCR-peptide/MHC interaction was "dominated" by the peptide.

Studying the mouse 2C TCR binding to the QL9 peptide presented by the class I MHC H2-L^d, Kranz and colleagues estimated that 37% of the binding energy results from recognition of peptide, whereas 63% results from recognition of the MHC (48, 49). Similar results were obtained for 2C TCR recognition of the SIYR peptide presented by H2-K^b (50). In both cases, these authors also found the largest contributions stem from CDR loops 1 and 2. However, unlike here, in which we mutated MHC positions contacted by the TCR, the results in the 2C system stem from mutational analysis of the T cell receptor. Furthermore, contact residues were predicted from molecular models based on the structure of the 2C TCR complexed with H-$2K^b$ presenting the dEV8 peptide (3, 48). Nevertheless, the results in the 2C system appear to contradict ours, which imply a larger role for the peptide and by extension, the CDR3 loops which generally form most TCR-peptide contacts. As Kranz and colleagues suggested (49, 50), this may reflect differences in CDR3 loop length between the 2C and A6 TCRs, the latter of which are longer. This may be one mechanism by which the peptide influences TCR focus, as recognition of a given peptide may require common TCR features (such as CDR3 loop length and flexibility). Peptide conformation may require subtle shifts in the geometry of the bound TCR, such that smaller loops are unable to contact peptide/MHC. For example, the Vβ CDR1 and CDR2 loops of the A6 TCR do not contact Tax/HLA-A2, whereas all Vβ and Vα loops contact ligand in the structure of the 2C TCR complexed with two different peptides presented by H-$2K^b$ (3, 6). Recognition of Tax/HLA-A2 also requires a conformational change in the peptide (2, 4), which may contribute to the apparently large contributions made by the peptide and CDR3 loops as well as diminish the contributions made through other positions. Based on these considerations, different energetic footprints might well be expected with different TCR-peptide/MHC interactions.

The 65/66/69 region is not the exclusive location of the functional footprint on HLA-A2, as TCRs that are specific for other HLA-A2–presented peptides are in some cases sensitive to other sets of residues. We readily found alloreactive T cell lines as well as T cell lines specific for the influenza M1 58–66 peptide that were unaffected by either of the R65A, K66A, and A69G mutations (preliminary results suggest that position 155 is important for recognition of HLA-A2 with the M1 peptide). Similar results have been observed in other systems; for example, Ono et al. (45) also observed that changes in the peptide altered TCR reactivity towards a panel of MHC mutants. Thus, there is little evidence that any class I MHC residues evolved to "hold" or "direct" the TCR into position, as TCRs of different peptide specificity do not appear to focus on the same region of the MHC.

We thank Dr. J. Hennecke and other members of the Wiley/Harrison groups for insightful discussion, A. Haykov for technical assistance, and members of the Strominger group at Harvard University for access to a Biacore 2000 instrument.

This work was supported by the National Institutes of Health and Howard Hughes Medical Institute. B.M. Baker is supported by a postdoctoral fellowship from the Cancer Research Institute. D.C. Wiley is an investigator of the Howard Hughes Medical Institute.

Submitted: 26 September 2000
Revised: 19 December 2000
Accepted: 23 January 2001

References

1. Garcia, K., M. Degano, R. Stanfield, A. Brunmark, M. Jackson, P. Peterson, L. Teyton, and I. Wilson. 1996. An αβ T cell receptor structure at 2.5 Å and its orientation in the TCR-MHC complex. *Science.* 274:209–219.
2. Garboczi, D., P. Ghosh, U. Utz, Q. Fan, W. Biddison, and D.C. Wiley, 1996. Structure of the complex between human T-cell receptor, viral peptide and HLA-A2. *Nature.* 384:134–141.
3. Garcia, K., M. Degano, L. Pease, M. Huang, P. Peterson, L. Teyton, and I. Wilson. 1998. Structural basis of plasticity in T cell receptor recognition of a self peptide-MHC antigen. *Science.* 279:1166–1172.
4. Ding, Y.-H., K. Smith, D. Garboczi, U. Utz, W. Biddison, and D.C. Wiley. 1998. Two human T cell receptors bind in a similar diagonal mode to the HLA- A2/Tax peptide complex using different TCR amino acids. *Immunity.* 8:403–411.
5. Ding, Y.-H., B.M. Baker, D. Garboczi, W. Biddison, and D.C. Wiley. 1999. Four A6-TCR/peptide/HLA-A2 structures that generate very different T cell signals are nearly identical. *Immunity.* 11:45–56.
6. Degano, M., K. Garcia, V. Apostolopoulos, M. Rudolph, L. Teyton, and I. Wilson. 2000. A functional hot spot for antigen recognition in a superagonist TCR/MHC complex. *Immunity.* 12:251–261.
7. Reiser, J.-B., C. Darnault, A. Guimezanes, C. Gregoire, T. Mosser, A.-M. Schmitt-Verhulst, J. Fontecilla-Camps, B. Malissen, D. Housset, and G. Mazza. 2000. Crystal structure of a T cell receptor bound to an allogeneic MHC molecule. *Nat. Immunol.* 1:291–297.
8. Reinherz, E., K. Tan, L. Tang, P. Kern, J. Liu, Y. Xiong, R. Hussey, A. Smolyar, B. Hare, R. Zhang, et al. 1999. The crystal structure of a T cell receptor in complex with peptide and MHC class II. *Science.* 286:1913–1921.
9. Sun, R., S. Shepherd, S. Geier, C. Thomson, J. Sheil, and S. Nathenson. 1995. Evidence that the antigen receptors of cytotoxic T lymphocytes interact with a common recognition pattern on the H-$2K^b$ molecule. *Immunity.* 3:573–582.
10. Smith, K., and C. Lutz. 1997. Alloreactive T cell recognition of MHC class I molecules: the T cell receptor interacts with limited regions of the MHC class I long α helices. *J. Immunol.* 158:2805–2812.
11. Hornel, T., J. Solheim, N. Myers, W. Gillanders, G. Balendiran, T. Hansen, and J. Connolly. 1999. Alloreactive and syngeneic CTL are comparably dependent on interaction with MHC class I α-helical residues. *J. Immunol.* 163:3217–3225.
12. Cunningham, B., and J. Wells. 1989. High-resolution epitope mapping of hGH-receptor interactions by alanine-scanning mutagenesis. *Science.* 244:1081–1085.
13. Winter, C., B. Carreno, R. Turner, S. Koenig, and W. Biddison. 1991. The 45 pocket of HLA-A2.1 plays a role in pre-

sentation of influenza virus matrix peptide and alloantigens. *J. Immunol.* 146:3508–3512.
14. Ho, S., H. Hunt, R. Horton, J. Pullen, and L. Pease. 1989. Site-directed mutagenesis by overlap extension using the polymerase chain reaction. *Gene.* 77:51–59.
15. Long, E., S. Rosen-Bronson, D. Karp, M. Malnati, R. Sekaly, and D. Jaraquemada. 1991. Efficient cDNA expression vectors for stable and transient expression of HLA-DR in transfected fibroblast and lymphoid cells. *Hum. Immunol.* 31:229–235.
16. Storkus, W., D. Howell, R. Salter, J. Dawson, and P. Cresswell. 1987. NK susceptibility varies inversely with target cell class I HLA antigen expression. *J. Immunol.* 138:1657–1659.
17. Sanots-Aguado, J., J. Barbosa, P. Biro, and J. Strominger. 1988. Molecular characterization of serologic recognition sites in the human HLA-A2 molecule. *J. Immunol.* 141:2811–2818.
18. Lombardi, G., M. Matsui, R. Moots, G. Aichinger, S. Sidhu, R. Batchelor, J. Frelinger, and R. Lechler 1991. Limited regions of the alpha-2 domain alpha-helix control anti-A2 allorecognition: an analysis using a panel of A2 mutants. *Immunogenetics.* 34:149–156.
19. Krangel, M., S. Taketani, D. Pious, and J. Strominger. 1983. HLA-A2 mutants immunoselected in vitro. Definition of residues contributing to an HLA-A2–specific serological determinant. *J. Exp. Med.* 157:324–336.
20. Ways, J., J. Rothbard, and P. Parham. 1986. Amino acid residues 56 to 69 of HLA-A2 specify an antigenic determinant shared by HLA-A2 and HLA-B17. *J. Immunol.* 137:217–222.
21. Garboczi, D., D. Hung, and D.C. Wiley. 1992. HLA-A2-peptide complexes: refolding and crystallization of molecules expressed in *Escherichia coli* and complexed with single antigenic peptides. *Proc. Natl. Acad. Sci. USA.* 89:3429–3433.
22. MacFerrin, K., M. Terranova, S. Schreiber, and G. Verdine. 1990. Overproduction and dissection of proteins by the expression cassette polymerase chain reaction. *Proc. Natl. Acad. Sci. USA.* 87:1937–1941.
23. Garboczi, D., U. Utz, P. Ghosh, A. Seth, J. Kim, E. VanTienhoven, W. Biddison, and D.C. Wiley. 1996. Assembly, specific binding, and crystallization of a human TCR-$\alpha\beta$ with an antigenic Tax peptide from human T lymphotropic virus type 1 and the class I MHC molecule HLA-A2. *J. Immunol.* 157:5403–5410.
24. O'Shea, E., K. Lumb, and P. Kim. 1993. Peptide "velcro": design of a heterodimeric coiled coil. *Curr. Biol.* 3:658–667.
25. Pace, C., F. Vajdos, L. Fee, G. Grimsley, and T. Gray. 1995. How to measure and predict the molar absorption coefficient of a protein. *Protein Sci.* 4:2411–2423.
26. Utz, U., D. Banks, S. Jacobson, and W. Biddison. 1996. Analysis of the T-cell receptor repertoire of human T-cell leukemia virus type 1 (HTLV-1) Tax-specific $CD8^+$ cytotoxic T lymphocytes from patients with HTLV-1-associated disease: evidence for oligoclonal expansion. *J. Virol.* 70:843–851.
27. Gotch, F., J. Rothbard, K. Howland, A. Townsend, and A. McMichael. 1987. Cytotoxic T lymphocytes recognize a fragment of influenza virus matrix protein in association with HLA-A2. *Nature.* 326:881–882.
28. Utz, U., S. Koenig, J. Coligan, and W. Biddison. 1992. Presentation of three different viral peptides, HTLV-1 Tax, HCMV gB, and influenza virus M1 is determined by common structural features of the HLA-A2.1 molecule. *J. Immunol.* 149:214–221.
29. Mattson, D., N. Shimojo, E. Cowan, J. Baskin, R. Turner, B. Shvetsky, J. Coligan, W. Maloy, and W. Biddison. 1989. Differential effects of amino acid substitutions in the beta sheet floor and alpha two helix of HLA-A2 on recognition by alloreactive versus viral peptide-specific CTL. *J. Immunol.* 143:1101–1107.
30. Morgan, C., J. Holton, B. Olafson, P. Bjorkman, and S. Mayo. 1997. Circular dichroism determination of class I MHC-peptide equilibrium dissociation constants. *Protein Sci.* 6:1771–1773.
31. Khan, A., B. Baker, P. Ghosh, W. Biddison, and D.C. Wiley. 2000. The structure and stability of an HLA-A*0201/octameric tax peptide complex with an empty conserved peptide-N-terminal binding site. *J. Immunol.* 164:6398–6405.
32. Garboczi, D., and W. Biddison. 1999. Shapes of MHC restriction. *Immunity.* 10:1–7.
33. Sloan-Lancaster, J., A. Shaw, J. Rothbard, and P. Allen. 1994. Partial T cell signaling: altered phospho-zeta and lack of ZAP-70 recruitment in APL-induced T cell anergy. *Cell.* 79:913–922.
34. Madrenas, J., R. Wange, J. Isakov, L. Samelson, and R. Germain. 1995. Zeta phosphorylation without ZAP-70 activation induced by TCR antagonists or partial agonists. *Science.* 267:515–518.
35. Clackson, T., and J. Wells. 1995. A hot spot of binding energy in a hormone-receptor interface. *Science.* 267:383–386.
36. Cunningham, B., and J. Wells. 1993. Comparison of a structural and a functional epitope. *J. Mol. Biol.* 234:554–563.
37. Wells, J. 1996. Binding in the growth hormone receptor complex. *Proc. Natl. Acad. Sci. USA.* 93:1–6.
38. Baker, B.M., S. Gagnon, W. Biddison, and D.C. Wiley. 2000. Conversion of a T cell antagonist into an agonist by repairing a defect in the TCR/peptide/MHC interface: Implications for TCR signaling. *Immunity.* 13:475–484.
39. Davis, M., J. Boniface, Z. Reich, D. Lyons, J. Hampl, B. Arden, and Y. Chien. 1998. Ligand recognition by alpha beta T cell receptors. *Annu. Rev. Immunol.* 16:523–544.
40. Manning, T., and D.M. Kranz. 1999. Binding energetics of T cell receptor variable region residues: correlation with immunological consequences. *Immunol. Today.* 20:417–422.
41. Janin, J. 1997. The kinetics of protein-protein recognition. *Proteins.* 28:153–161.
42. Selzer, T., S. Albeck, G. Schreiber. 2000. Rational design of faster associating and tighter binding protein complexes. *Nat. Struct. Biol.* 7:537–541.
43. Fersht, A. 1999. Structure and Mechanism in Protein Science: A Guide to Enzyme Catalysis and Protein Folding. W. H. Freeman & Co, New York. 475 pp.
44. Alam, S., P. Travers, J. Wung, W. Nasholds, S. Redpath, S. Jameson, and N. Gascoigne. 1996. T-cell-receptor affinity and thymocyte positive selection. *Nature.* 381:616–620.
45. Ono, T., T. DiLorenzo, F. Wang, A. Kalergis, and S. Nathenson. 1998. Alterations in TCR-MHC contacts subsequent to cross-recognition of class I MHC and singly substituted peptide variants. *J. Immunol.* 161:5454–5463.
46. Hausmann, S., W. Biddison, K. Smith, Y.-H. Ding, D. Garboczi, U. Utz, D.C. Wiley, and K. Wucherpfennig. 1999. Peptide recognition by two HLA-A2/Tax_{11-19}-specific T cell clones in relationship to their MHC/peptide/TCR crystal structures. *J. Immunol.* 162:5389–5397.
47. Ehrich, E., B. Devaux, E. Rock, J. Jorgensen, M. Davis, and Y. Chien. 1993. T-cell receptor interaction with peptide major histocompatibility complex (MHC) and superantigen

MHC ligands is dominated by antigen. *J. Exp. Med.* 178: 713–722.
48. Speir, J., K. Garcia, A. Brunmark, M. Degano, P. Peterson, L. Teyton, and I. Wilson. 1998. Structural basis of 2C TCR allorecognition of H-2L^d peptide complexes. *Immunity*. 8:553–562.
49. Manning, T., C. Schlueter, T. Brodnick, E. Parke, J. Speir, K. Garcia, L. Teyton, I. Wilson, and D.M. Kranz. 1998. Alanine scanning mutagenesis of an αβ T cell receptor: mapping the energy of antigen recognition. *Immunity*. 8:413–425.
50. Lee, P., H. Churchill, M. Daniels, S. Jameson, and D.M. Kranz. 2000. Role of 2C T cell receptor residues in the binding of self- and allo-major histocompatibility complexes. *J. Exp. Med.* 191:1355–1364.